Translational Oncology
www.transonc.com

Volume 4 Number 5 October 2011 pp. 282–292 282

Role of $\alpha_5\beta_1$ Integrin Up-regulation in Radiation-Induced Invasion by Human Pancreatic Cancer Cells[1]

Hongren Yao*, Zhao-Zhu Zeng*, Kevin S. Fay*, Donna M. Veine*, Evan D. Staszewski*, Meredith Morgan*, Kari Wilder-Romans*, Terence M. Williams*, Aaron C. Spalding†, Edgar Ben-Josef* and Donna L. Livant*

*Department of Radiation Oncology, University of Michigan, Ann Arbor, MI, USA; †Norton Cancer Radiation Center, Louisville, KY, USA

Abstract

Radiotherapy is used in the management of pancreatic cancer because of its high propensity for locoregional relapse: one third of patients succumb to localized disease. Thus, strategies to improve the efficacy of radiotherapy in pancreatic cancer are important to pursue. We used naturally serum-free, selectively permeable basement membranes and confocal microscopy of fluorescent antibody–stained human Panc-1, MiaPaCa-2, and BxPC-3 pancreatic cancer cell lines to investigate the effects of ionizing radiation on $\alpha_5\beta_1$ integrin fibronectin receptor expression and on $\alpha_5\beta_1$-mediated invasion. We report that radiation rapidly induces pancreatic cancer cell invasion, and that radiation-induced invasion is caused by up-regulation of $\alpha_5\beta_1$ integrin fibronectin receptors by transcriptional and/or postendocytic recycling mechanisms. We also report that radiation causes $\alpha_5\beta_1$ up-regulation in Panc-1, MiaPaCa-2, and BxPC-3 tumor xenografts and that upregulated $\alpha_5\beta_1$ colocalizes with upregulated early or late endosomes in Panc-1 or BxPC-3 tumors, respectively, although it may colocalize significantly with both endosome types in MiaPaCa-2 tumors. Our results suggest that systemic inhibition of $\alpha_5\beta_1$-mediated invasion might be an effective way to reduce radiation-induced pancreatic cancer cell invasion, thereby improving the efficacy of radiotherapy.

Translational Oncology (2011) 4, 282–292

Introduction

Pancreatic cancer has a high predilection for both distant metastatic spread and for local relapse or progression. Local relapse after surgery or local progression of unresectable pancreatic cancer is common; approximately one third of patients actually succumb to localized disease [1]. Thus, to improve local control, radiotherapy is often used in addition to systemic therapies to treat this disease. Recent evidence suggests that the combination of radiation with chemotherapy improves survival compared with chemotherapy alone [2,3].

Radiation has numerous effects on adhesion molecules because it stimulates production of reactive oxygen intermediates [4]. For example, a single 3-Gy dose of gamma radiation has been shown to rapidly upregulate surface $\alpha v\beta_3$ and to stimulate glioma cell migration and invasion [5]. Radiation (2.5-5 Gy) has also been shown to upregulate surface $\alpha_5\beta_1$ integrin on COLO-320 colorectal carcinoma cells [6]. We have previously demonstrated that the $\alpha_5\beta_1$ integrin fibronectin receptor mediates invasion in cancer [7–9] and human microvascular endothelial cells (HMVECs) [10]. Matrix metalloproteinase 1 (MMP-1)–dependent invasion by metastatic prostate and breast cancer cells is induced when their constitutively activated $\alpha_5\beta_1$ integrin fibronectin receptors interact with the PHSRN sequence of the plasma fibronectin (pFn) cell binding domain [7–9]. The PHSRN-$\alpha_5\beta_1$ interaction also induces rapid α_5 messenger RNA (mRNA) and surface $\alpha_5\beta_1$ up-regulation, leading to increased MMP-1–dependent invasion by HMVEC; it also induces MMP-1–dependent invasion by fibroblasts and keratinocytes [10,11].

On the basis of our previous work demonstrating the importance of the $\alpha_5\beta_1$ integrin fibronectin receptor in invasion and the high

Address all correspondence to: Donna L. Livant, PhD, Department of Radiation Oncology, University of Michigan, Room 4424F Medical Science 1, 1301 Catherine St, Ann Arbor, MI 48109-5637. E-mail: dlivant@umich.edu

[1]This study was supported by National Institutes of Health grants R01 CA119007 (D.L. Livant), R03 CA 127050 (E. Ben-Josef). The authors have no commercial affiliations or financial interests that may be considered conflicts of interest.
Received 11 March 2011; Revised 9 May 2011; Accepted 16 May 2011

1944-7124/11/ DOI 10.1593/tlo.11133

invasive/metastatic potential of pancreatic cancers, we investigated the effects of ionizing radiation on $\alpha_5\beta_1$ expression and invasion in three human pancreatic cancer cell lines, *in vitro* and as tumors in athymic nude mice. When we found that radiation caused a rapid induction of $\alpha_5\beta_1$ integrin–mediated, pFn-dependent invasion, we proceeded to investigate the underlying mechanism(s). We hypothesized that the increase in radiation-induced invasion was mediated by transcriptionally or posttranslationally increased surface $\alpha_5\beta_1$ integrin. Postendocytic sorting of internalized membrane proteins is crucial for cell surface retrieval of receptors on ligand dissociation. To return directly to the plasma membrane in a "short loop," $\alpha_5\beta_1$ integrins can internalize to early endosomes [12]. Alternatively, they are transported to the perinuclear recycling compartment before recycling to the cell surface in a "long loop" involving trafficking through late endosomes [13]. Hence, we determined the effects of radiation on levels of early and late endosomes in Panc-1, MiaPaCa-2, and BxPC-3 cells by immunofluorescent (IF) staining.

To determine the mechanism(s) of radiation-induced invasion, we examined $\alpha_5\beta_1$ transcriptional regulation as well as both early and late endosome recycling of $\alpha_5\beta_1$. We report that radiation rapidly induced pFn-dependent, $\alpha_5\beta_1$ integrin–mediated invasion by Panc-1, MiaPaCa-2, and BxPC-3 cells *in vitro* and caused significant up-regulation of surface $\alpha_5\beta_1$ by increased α_5 transcription or by post-endocytic recycling from early (Panc-1) or from both early and late endosomes (BxPC-3 and MiaPaCa-2). We also report that radiation induced surface $\alpha_5\beta_1$ up-regulation in human Panc-1, MiaPaCa-2, and BxPC-3 tumors in athymic mice, with similar endosomal colocalization patterns as those observed in the cultured cells.

Materials and Methods

Cell Culture

BxPC-3 cells [14] (ATCC, Manassas, VA) were cultured in RPMI-1640 medium (Mediatech, Inc, Herndon, VA) in 10% fetal bovine serum (FBS), with 100 μg/ml streptomycin in 5% CO_2. Panc-1 cells [15] (ATCC) were cultured in Dulbecco modified Eagle medium (Invitrogen, Carlsbad, CA) with 100 μg/ml streptomycin in 10% FBS in 10% CO_2. MiaPaCa-2 cells [16] were cultured in Dulbecco modified Eagle medium (Invitrogen) with 100 μg/ml streptomycin in 10% FBS and 2.5% horse serum in 10% CO_2.

Irradiation of Cells and Tumors

Adherent cells were irradiated once with a single fraction of 1 to 4 Gy (Panc-1), 0.5 to 5.0 Gy (MiaPaCa-2), or 1 to 6 Gy (BxPC-3). Panc-1, MiaPaCa-2, and BxPC-3 tumors were each grown subcutaneously to 200 mm^3 in the flanks of athymic nude mice, using protocols approved by the University Committee on Use and Care of Animals. Before removal for histologic analysis, tumors of shielded mice were irradiated once per day for 5 days, at 2-Gy dosages. Irradiations were performed with a Philips RT250 orthovoltage unit (KIMTRON Medical, Woodbury, CT) at a 2-Gy/min dosage rate. Dosimetry was performed with an ionization chamber connected to an electrometer system, directly traceable to National Institute of Standards and Technology calibration.

In Vitro *Invasion Assays*

Naturally serum-free, selectively permeable sea urchin embryo basement membranes (SU-ECMs) were prepared, and *in vitro* invasion assays were performed as described [7–11]. Irradiated Panc-1, MiaPaCa-2, and BxPC-3 cells were incubated for various times after a single radiation dosage. Ten minutes before the end of the appropriate incubation period, irradiated cells were suspended, placed on SU-ECM basement membranes, and allowed to invade for 16 hours before scoring. Plasma fibronectin–depleted (pFn^-) FBS was made as described [7,8]. For *in vitro* invasion assays, 300 μg/ml blocking anti–$\alpha_5\beta_1$ integrin P1D6 monoclonal antibody (MAb), blocking anti–$\alpha_3\beta_1$ P1B5 MAb, COMY4A2 blocking anti–MMP-1 MAb, CA-4001 blocking anti–MMP-2 MAb, GE-213 blocking anti–MMP-9 MAb (Chemicon International, Temecula, CA), or appropriate isotype controls (Chemicon International) were prebound to suspended Panc-1, MiaPaCa-2, or BxPC-3 cells for 20 minutes on ice. Antibody-bound cells were pelleted, washed once, suspended in medium with 10% FBS, placed on SU-ECM, and incubated for 16 hours at 37°C before scoring at 400-fold magnification using a Nikon Diaphot inverted microscope (Mager Scientific, Dexter, MI) with phase-contrast optics, as described [7–11]. All experiments were performed in triplicate. Mean invasion percentages (±SD) were fit by cubic spline using GraphPad Prism 5 software (GraphPad Software, San Diego, CA).

Real-time Reverse Transcription—Polymerase Chain Reaction

Total RNA was isolated from irradiated Panc-1, MiaPaCa-2, and BxPC-3 cells 1 hour after radiation, using an RNeasy Plus Mini Kit (QIAGEN GmbH, Hilden, Germany). RNA integrity was assessed with Agilent 2100 Bioanalyser (Agilent Technologies, Waldbronn, Germany). One-step reverse transcription—polymerase chain reaction (RT-PCR) assays were performed using RT-PCR Kit (QIAGEN), as directed. Integrin α_5 and MMP-1 primers, and reaction conditions have been described previously [10,17]. Expression levels were normalized to glyceraldehyde 3-phosphate dehydrogenase primer reactions [18]. Data were collected using the ABI PRISM 7900HT Sequence Detection System (Applied Biosystems, Foster City, CA), and data analysis was performed with SDS 2.2.1 software (Applied Biosystems). Normalized expression was calculated using comparative threshold cycle (C_t), and fold changes were derived from the $2^{-\Delta\Delta Ct}$ values for α_5 and MMP-1. *P* values were calculated with Student's *t* test statistical program SPSS 15.0 (SPSS, Inc, Chicago, IL). All experiments were performed three times.

Immunofluorescent Staining of Panc-1, MiaPaCa-2, and BxPC-3 Cells

After irradiation, cells were incubated at 37°C for various times, rinsed thrice with phosphate-buffered saline (PBS), and fixed for 15 minutes in 4% paraformaldehyde in PBS at room temperature. Cells were treated with 10% normal goat serum (NGS; Vector Laboratories, Burlingame CA) in PBS with 0.2% Triton X-100 for 1 hour. After blocking, cells were incubated in a mixture of two affinity-purified primary antibodies: monoclonal antibody (MAb) P1D6 anti-$\alpha_5\beta_1$ (MAb1969), diluted 1:500, and rabbit polyclonal antiserum (RAb) anti–MMP-1 (RAB8105), diluted 1:400 (Chemicon International); or affinity-purified RAb anti–$\alpha_5\beta_1$ (RAB1928), diluted 1:500 (Chemicon); or anti–EEA-1 MAb or anti–LAMP-1 RAb (BD Biosciences, San Jose, CA) in 5% NGS in PBS and 0.25% Triton overnight at 4°C. After three PBS washes, cells were incubated in a mixture of antirabbit and antimouse secondary antibodies, conjugated with cyanine 3 (Cy3) or fluorescein isothiocyanate, respectively (Jackson

ImmunoResearch Lab, Inc) at 1:200 for 1 hour at room temperature. After three rinses in PBS, slides were mounted in Vectashield Mounting medium (Chemicon) with 4′,6′-diamidino-2-phenylindole (DAPI), sealed with nail polish, and examined using a confocal laser scanning microscope (LSM 510; Carl Zeiss MicroImaging, LLC, Thornwood, NY). Mean fluorescence intensities were calculated by using ImageJ software over 30 areas per treatment, selected randomly under a magnification of 400×. All experiments were performed three times. All data are expressed as mean ± SEM and evaluated with analysis of variance Student's *t* test. Significance was set at $P < .05$.

IF Staining of Tumor Xenografts

After fixation in 4% paraformaldehyde, tumors were cut into sections of 5-μm thickness with a Zeiss Cryostat; and sections were rinsed three times with PBS. After blocking with 10% NGS in PBS and Triton for 1 hour at room temperature, sections were incubated for 48 hours at 4°C with primary antibodies, as described previously. Anti–EEA-1 MAb, anti–LAMP-1 RAb, or anti–$\alpha_5\beta_1$ P1D6 MAb or anti–$\alpha_5\beta_1$ RAb was used at 1:200 dilutions. After three PBS rinses, sections were incubated in a mixture of antirabbit and antimouse secondary antibodies, conjugated with Cy3 or fluorescein isothiocyanate, respectively (Jackson ImmunoResearch Lab, Inc) at 1:200 dilutions for 1 hour at room temperature, as described above. Slides were mounted in Vectashield Mounting medium with DAPI, sealed with nail polish, and examined with a confocal laser scanning microscope (LSM 510; Carl Zeiss MicroImaging).

Sections with double immunostaining of anti–EEA-1 or –LAMP-1 and anti–$\alpha_5\beta_1$ primary antibodies were examined by confocal microscopy, under 400× magnification. Cells of Panc-1, MiaPaCa-2, or BxPC-3 tumors, with colocalized fluorescent immunostaining of both early or late endosomes and $\alpha_5\beta_1$ integrin, were counted as positive if they contained gold (red plus green) immunofluorescence in greater than 70% of their cytoplasmic area [19–22]. Fluorescence intensities of 20 randomly selected areas per section were quantified on each of 30 sections from each tumor by ImageJ analysis computer software. Sections were each separated by a distance of 50 μm; hence, a total of 600 areas distributed throughout a 1.5-mm thickness of tumor tissue were analyzed from each tumor. A total of nine irradiated and nine unirradiated Panc-1, BxPC-3, and MiaPaCa-2 tumors were sampled. All data are expressed as mean ± SEM and evaluated with analysis of variance Student's *t* test. Significance was set at $P < .05$. Image analysis of edge (0-75 μm) *versus* middle (150-300 μm) of sectioned, radiated, and unirradiated Panc-1, MiaPaCa-2, and BxPC-3 tumors was performed by confocal microscopy. Tumor edges were defined by the presence of microvasculature and/or associated connective tissue. Distances from tumor edges were measured by software included in the confocal laser scanning microscope (LSM 510; Carl Zeiss MicroImaging, LLC).

Results

Dependence of Radiation-Induced Invasion on pFn and $\alpha_5\beta_1$ Integrin

To begin determination of the effects of radiation on invasion, we measured the ability of Panc-1, MiaPaCa-2, and BxPC-3 cells to invade basement membranes in response to radiation. We found that invasion was significantly increased 1 hour after irradiation at various dosages, as shown in Figure 1*A*. Maximal Panc-1 invasion occurred after a 2-Gy dose, whereas 3 Gy induced maximal invasion by MiaPaCa-2 and BxPC-3 cells. Increased Panc-1 invasion was also observed after 1 or 3 Gy, and 2 Gy also increased invasion by MiaPaCa-2 and BxPC-3 cells. At higher doses, the percentages of invaded cells declined. We also evaluated the kinetics of invasion induction in response to radiation, using 2 (Panc-1) or 3 Gy (MiaPaCa-2 and BxPC-3). Peak invasion induction occurred 1 hour after irradiation for all three cell lines (Figure 1*B*). Invasiveness was still elevated after 90 minutes and returned to baseline levels within 2 to 3 hours after radiation. Given the known role of MMP-1 in $\alpha_5\beta_1$-mediated invasion, the roles of pFn, $\alpha_5\beta_1$, and MMP-1 in radiation-induced invasion by Panc-1, MiaPaCa-2, and BxPC-3 cells were evaluated. Selective depletion of pFn from serum prevented radiation-induced invasion, whereas adding pFn back at the concentration expected in 10% serum [7,8] fully restored it (Figure 1*C*). Consistent with the pFn requirement, prebinding irradiated Panc-1, MiaPaCa-2, and BxPC-3 cells to blocking anti–$\alpha_5\beta_1$ MAb, before placement on SU-ECM, prevented radiation-induced invasion. Also, anti–MMP-1 prebinding prevented radiation-induced invasion, whereas prebinding to blocking anti–MMP-2 or –MMP-9 MAb had no inhibitory effect (Figure 1*C*). Taken together, these results suggest that radiation induces $\alpha_5\beta_1$-mediated invasion by pancreatic cancer cells, by increasing the expression of activated $\alpha_5\beta_1$, and that MMP-1 may play a key role in invasion.

Surface $\alpha_5\beta_1$ Integrin Up-regulation after Irradiation

The dependence of radiation-induced invasion on pFn, $\alpha_5\beta_1$, and MMP-1 suggests that radiation may cause rapid up-regulation of surface $\alpha_5\beta_1$ integrin fibronectin receptors and MMP-1 interstitial collagenase. We tested this hypothesis by fluorescent immunostaining of Panc-1, MiaPaCa-2, and BxPC-3 cells with anti-$\alpha_5\beta_1$ or anti–MMP-1 MAb 1 hour after irradiation with 2 (Panc-1) or 3 Gy (MiaPaCa-2 and BxPC-3). We found anti-$\alpha_5\beta_1$ immunofluorescence levels to be increased significantly in response to radiation in Panc-1, MiaPaCa-2, and BxPC-3 cells (Figure 2*A*). Quantitation of the anti-$\alpha_5\beta_1$ immunofluorescence levels in radiated and unirradiated cells revealed mean increases (±SD) of 2.2-fold (±0.1), 4.1-fold (±0.6), or 1.9-fold (±0.1) in surface $\alpha_5\beta_1$ for Panc-1, MiaPaCa-2, and BxPC-3 cells, respectively (shown in Figure 2*B*). As expected from the dependence of pFn-induced $\alpha_5\beta_1$-mediated invasion on MMP-1 in breast and prostate cancer [7,8] and of pFn cell-binding domain-induced $\alpha_5\beta_1$-mediated invasion on MMP-1 in microvascular cells [10], irradiated Panc-1, MiaPaCa-2 ,and BxPC-3 cells also displayed increased surface MMP-1, colocalized with $\alpha_5\beta_1$ integrin 1 hour after irradiation (Figure 2*A*). Quantitation of the anti–MMP-1 levels in radiated and unirradiated cells revealed 1.6-fold (±0.1), 1.4-fold (±0.2), or 2.1-fold (±0.2) mean (±SD) increases in surface MMP-1 for Panc-1, MiaPaCa-2, and BxPC-3 cells (Figure 2*C*).

Effects of Radiation on α_5 Integrin and MMP-1 mRNA Levels in Irradiated Panc-1, MiaPaCa-2, and BxPC-3 Cells

Radiation-induced $\alpha_5\beta_1$ up-regulation may be caused by increased α_5 integrin mRNA or by posttranscriptional processes. Hence, the effects of radiation on α_5 mRNA levels were evaluated by RT-PCR. Radiation caused significant up-regulation of α_5 mRNA levels in MiaPaCa-2 (2.6 ± 0.2-fold) and BxPC-3 (3.5 ± 1.0-fold) but not in irradiated Panc-1 cells (1.6 ± 0.6-fold; Figure 3). As expected from $\alpha_5\beta_1$-mediated up-regulation of MMP-1 mRNA in HMVEC [10], and dependence of $\alpha_5\beta_1$-mediated invasion on MMP-1 [7–11], we

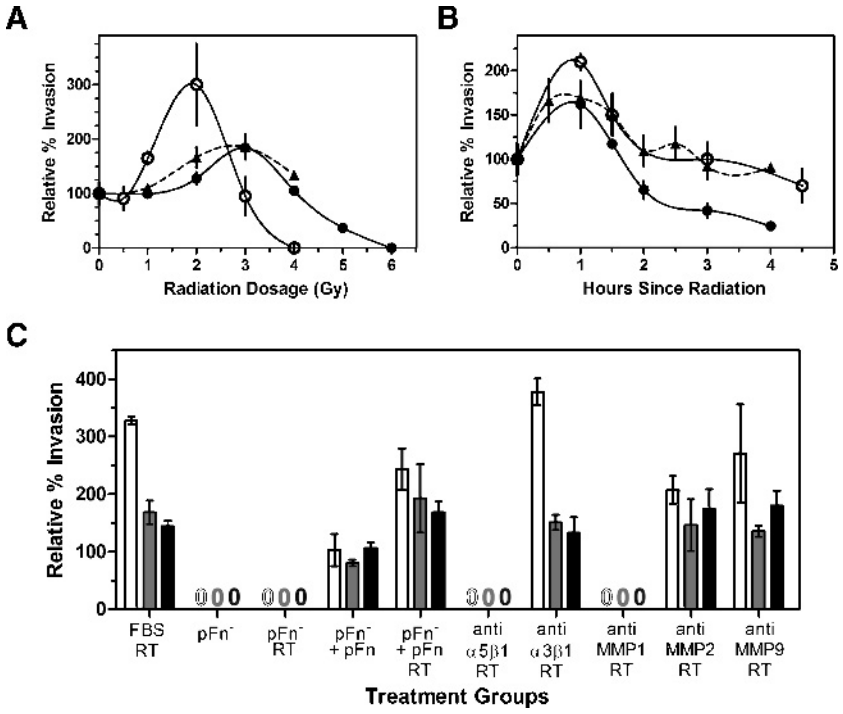

Figure 1. Radiation-induced invasion dose responses, time courses and dependence on pFn, $\alpha_5\beta_1$ integrin, and MMP-1. (A) Dose responses. *x* axis indicates radiation doses (Gy); *y* axis, relative percent invasion compared with unirradiated controls. Black circles indicate BxPC-3; black triangles, MiaPaCa-2; white circles, Panc-1. (B) Time courses. Doses: Panc-1, 2 Gy; MiaPaCa-2, 3 Gy; BxPC-3, 3 Gy. *x* axis indicates hours because radiation; *y* axis, relative percent invasion compared with unirradiated controls. Black circles indicate BxPC-3; black triangles, MiaPaCa-2; white circles, Panc-1. (C) pFn, $\alpha_5\beta_1$, and MMP-1 dependence. *x* axis indicates treatment groups. pFn, 5 μg/ml; FBS, 10%; anti-$\alpha_5\beta_1$, 300 μg/ml; anti-$\alpha_3\beta_1$, 300 μg/ml; anti–MMP-1, 100 μg/ml; anti–MMP-2, 100 μg/ml; anti–MMP-9, 100 μg/ml. *y* axis indicates relative percent invasion compared with unirradiated controls. Black bars indicate BxPC-3; gray bars, MiaPaCa-2; white bars, Panc-1. (A–C) Data are normalized to unirradiated controls and are the means ± first SDs of values from $n = 3$ experiments, each run in triplicate. Significance was set at $P < .05$.

found that radiation caused rapid up-regulation of MMP-1 mRNA levels in Panc-1 (3.0 ± 1.2-fold), MiaPaCa-2 (2.4 ± 0.3-fold), and BxPC-3 (3.5 ± 0.3-fold). Because α_5 transcription increased significantly ($P < .05$) in MiaPaCa-2 and BxPC-3 but not in Panc-1, whereas surface $\alpha_5\beta_1$ receptor levels increased 1.9- to 4.1-fold in all three cell lines, posttranscriptional mechanisms involving increases in trafficking rates may also be important, especially in Panc-1 cells.

Effects of Radiation on Early and Late Endosomes and Colocalization of Anti-α_5 Immunostaining in Panc-1, MiaPaCa-2, and BxPC-3 Cells

Integrins are continuously recycled through two distinct pathways. Rapid recycling occurs from early endosomes; however, recycling receptors may also return to the plasma membrane from the late endosome perinuclear compartment, which may also contain newly translated proteins [12,23,24]. Hence, we assessed the effects of radiation on levels of early and late endosomes and on their colocalization of $\alpha_5\beta_1$. To determine the effects of radiation on levels of early and late endosome recycling of $\alpha_5\beta_1$, we coimmunostained in Panc-1, MiaPaCa-2, and BxPC-3 cells for early (EEA-1) or late (LAMP-1) endosomes and $\alpha_5\beta_1$. We observed that early endosome levels increased by 28-fold in Panc-1 and by 18-fold in MiaPaCa-2 cells 1 hour after radiation (Figure 4, *A* and *B*). More importantly, fluorescent anti-$\alpha_5\beta_1$ seemed to colocalize with anti–EEA-1 immunostaining. A significantly smaller radiation-induced increase in anti–EEA-1 (2.4-fold) was observed in BxPC-3 cells in response to radiation. In contrast, the radiation-induced increase in anti–LAMP-1 immunostaining of late endosomes in BxPC-3 cells (13.9-fold) was significantly greater than in Panc-1 (2.6-fold) or MiaPaCa-2 cells (3.6-fold; Figure 4, *A* and *C*). Consistent with late endosome recycling of $\alpha_5\beta_1$ in BxPC-3 cells, fluorescent anti-$\alpha_5\beta_1$ seemed to colocalize with anti–LAMP-1 immunostaining. Together, these data indicate that radiation may cause pronounced up-regulation of surface $\alpha_5\beta_1$ by increasing its recycling through early endosomes, without a significant increase or with only a modest increase α_5 subunit mRNA in Panc-1 and MiaPaCa-2 cells, respectively. In contrast, increased α_5 mRNA, as well as increased trafficking through late endosomes, may function in radiation-induced surface $\alpha_5\beta_1$ up-regulation in BxPC-3 cells. Because late endosomes, but not early endosomes, can contain newly translated proteins [13], these results are consistent with the increased α_5 mRNA levels we observed in MiaPaCa-2 and BxPC-3 cells in response to radiation.

Effects of Primacrine on Radiation-Induced Surface $\alpha_5\beta_1$ Up-regulation and Invasion in Panc-1, MiaPaCa-2, and BxPC-3 Cells

To further characterize the temporal changes in early and late endosomes induced by single radiation dosages, the effects on levels of early and late endosomes and surface $\alpha_5\beta_1$ integrin were determined by fluorescent immunostaining of Panc-1 cells 1, 2, and

4 hours after irradiation. Furthermore, to determine the involvement of endosome recycling on increased surface $\alpha_5\beta_1$, cells were treated with primacrine, an inhibitor of early endosomal recycling to the plasma membrane [25]. As shown by anti–EEA-1 immunostaining of Panc-1 cells 1, 2, or 4 hours after radiation, a rapid 28- to 35-fold up-regulation of early endosomes and an 11- to 14-fold increase surface $\alpha_5\beta_1$ were observed (Figure 5*A*). However, there was only a modest effect on the levels of late endosomes (1.8- to 3.1-fold increase). Consistent with these results, exposure of Panc-1 cells to primacrine shortly before irradiation prevented radiation-induced up-regulation of both early endosomes and surface $\alpha_5\beta_1$, with respect to unirradiated Panc-1 cells, as shown in Figure 5*A*.

Likewise in MiaPaCa-2 cells, up-regulation of early endosomes was evidenced by a rapid increase (18- to 22-fold) in anti–EEA-1 immunostaining in response to radiation. Furthermore, this increase in early endosomes was paralleled by a 13- to 21-fold increase surface $\alpha_5\beta_1$ (Figure 5*A*). Exposure of MiaPaCa-2 cells to primacrine shortly before irradiation prevented radiation-induced up-regulation of early endosomes (decrease to 0.6-fold of untreated levels). However, in contrast to Panc-1 cells, radiation also induced a significant

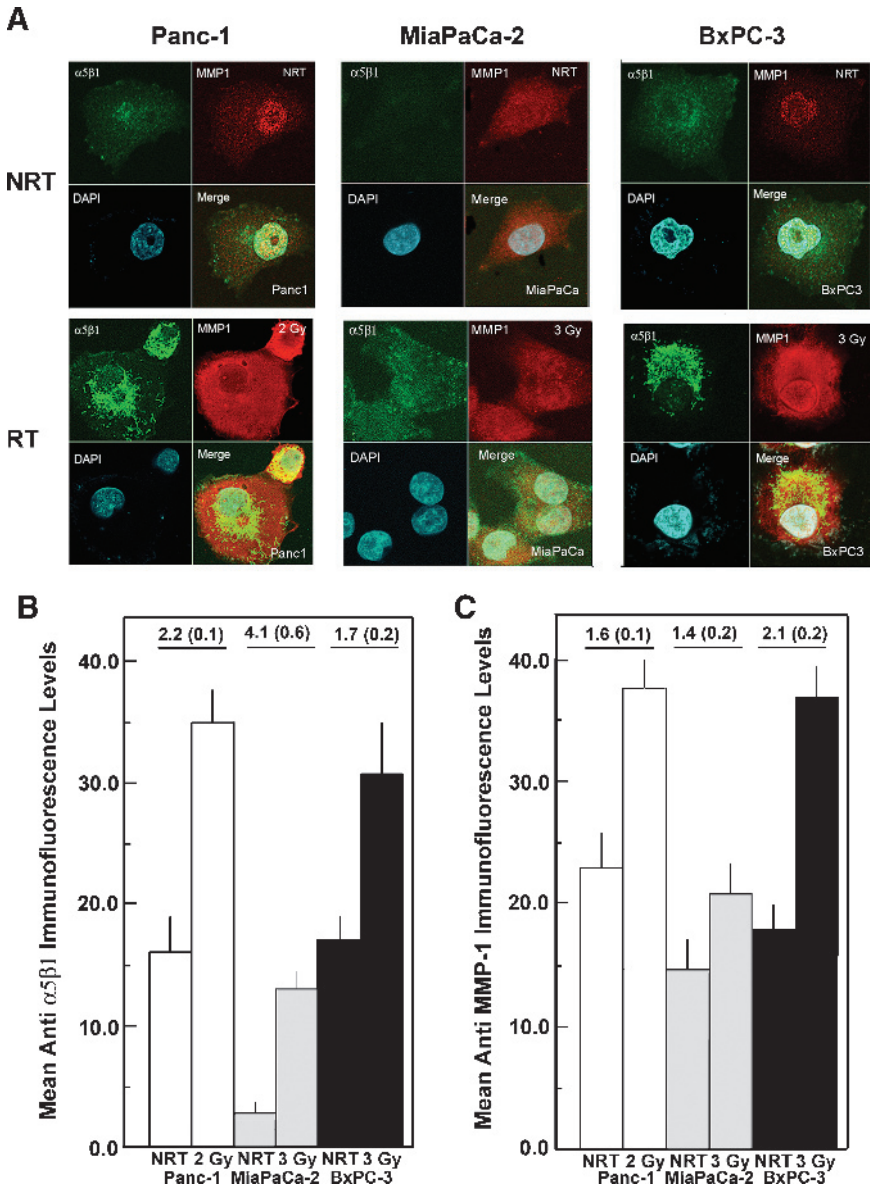

Figure 2. Radiation-induced surface $\alpha_5\beta_1$ and MMP-1 up-regulation. Panc-1, MiaPaCa-2, and BxPC-3 cells were treated with the indicated doses of radiation (RT) or without (NRT) and then fixed and stained with primary antibodies recognizing $\alpha_5\beta_1$ or MMP-1, fluorescent secondary antibodies, and DAPI. (A) Representative examples. $\alpha_5\beta_1$ indicates anti-$\alpha_5\beta_1$; DAPI, nuclear DNA; MMP1, anti–MMP-1; NRT, no radiation treatment; RT, 1 hour after radiation. (B) Anti-$\alpha_5\beta_1$ IF levels from three experiments. *x* axis indicates treatments and cell lines: 2 Gy, Panc-1; 3 Gy, MiaPaCa-2, 3 Gy, BxPC-3. NRT indicates no radiation treatment. *y* axis indicates mean anti-$\alpha_5\beta_1$ IF levels (±SEM). Mean fold up-regulation of surface immunofluorescence levels in irradiated *versus* unirradiated cells (±SD) are indicated. Significance was set at $P < .05$. (C) Anti–MMP-1 IF levels from three experiments. *x* axis indicates treatments and cell lines: 2 Gy, Panc-1; 3 Gy, MiaPaCa-2, 3 Gy, BxPC-3. NRT indicates no radiation treatment. *y* axis indicates mean anti–MMP-1 immunofluorescence levels (±SEM). Mean fold up-regulation (±SD) are shown at the top. $P < .05$.

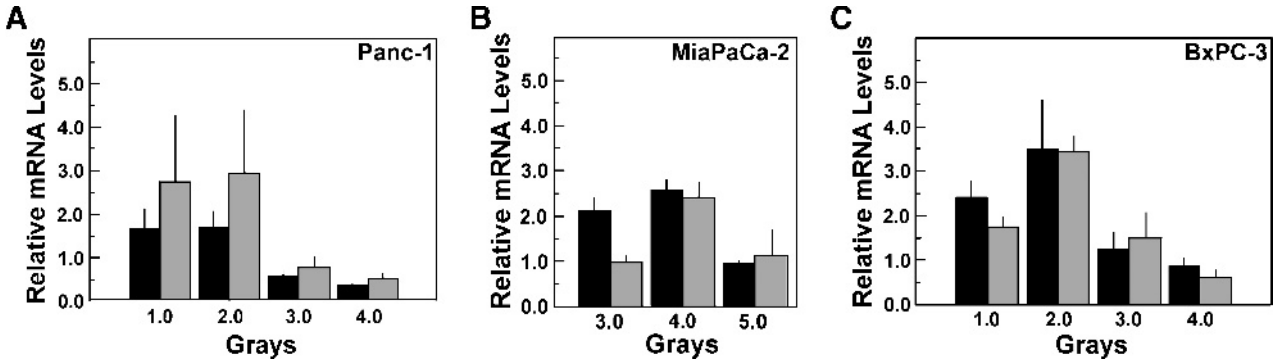

Figure 3. Effects of radiation on α_5 integrin subunit and MMP-1 mRNA levels: Panc-1 (A), MiaPaCa-2 (B), and BxPC-3 cells (C). *x* axes indicate dose in gray; *y* axes, mean relative mRNA levels (±SEM) for experiments run and repeated in triplicate. Black bars indicates α_5 mRNA; gray bars, MMP-1 mRNA. Significance was set at $P < .05$.

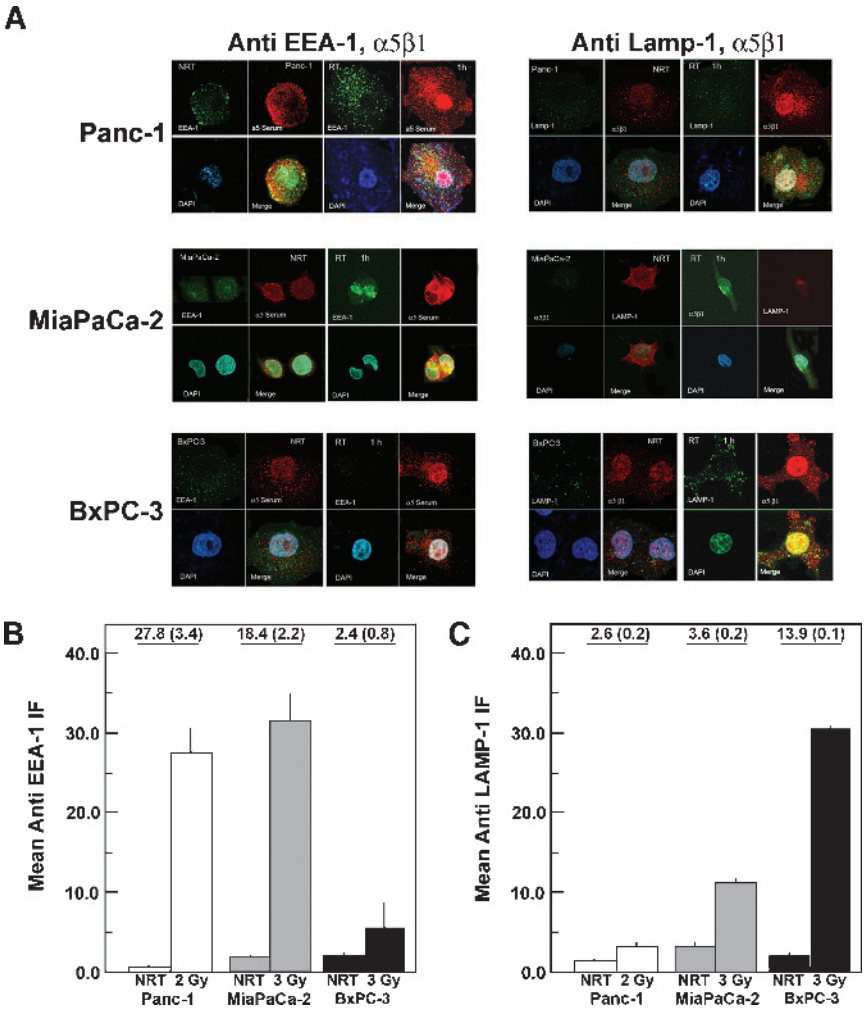

Figure 4. Effects of radiation on anti–EEA-1 and anti–LAMP-1 immunostaining and colocalization with anti-$\alpha_5\beta_1$. (A) Examples of unirradiated and radiated Panc-1, MiaPaCa-2, and BxPC-3 cells coimmunostained with anti–EEA-1 MAb (EEA-1) and anti-$\alpha_5\beta_1$ antiserum (α5 Serum) or with anti–LAMP-1 MAb (LAMP-1) and anti-$\alpha_5\beta_1$ MAb ($\alpha_5\beta_1$). (B) Effects of radiation on anti–EEA-1 IF levels. Black bars indicate BxPC-3; gray bars, MiaPaCa-2; white bars, Panc-1. All values listed were each made on four plates containing hundreds of cells, for each of two independent experiments. *x* axis indicates treatments and cell lines. NRT indicates no radiation treatment; 2GY, 1 hour after a single 2-Gy dose; 3GY, 1 hour after a single 3-Gy dose. *y* axis indicates mean anti–EEA-1 IF (±SEM). Mean fold up-regulation (±SD) shown at the top. Significance was set at $P < .05$. (C) Effects of radiation on anti–LAMP-1 IF. Black bars indicate BxPC-3; gray bars, MiaPaCa-2; white bars, Panc-1. All values listed were each made on four plates containing hundreds of cells, for each of two independent experiments. *x* axis indicates treatments and cell lines. NRT indicates no radiation treatment; 2GY, 1 hour after a single 2-Gy dose; 3GY, 1 hour after a single 3-Gy dose. *y* axis indicates mean anti–LAMP-1 IF (±SEM). Mean fold up-regulation (±SD) shown at the top. $P < .05$.

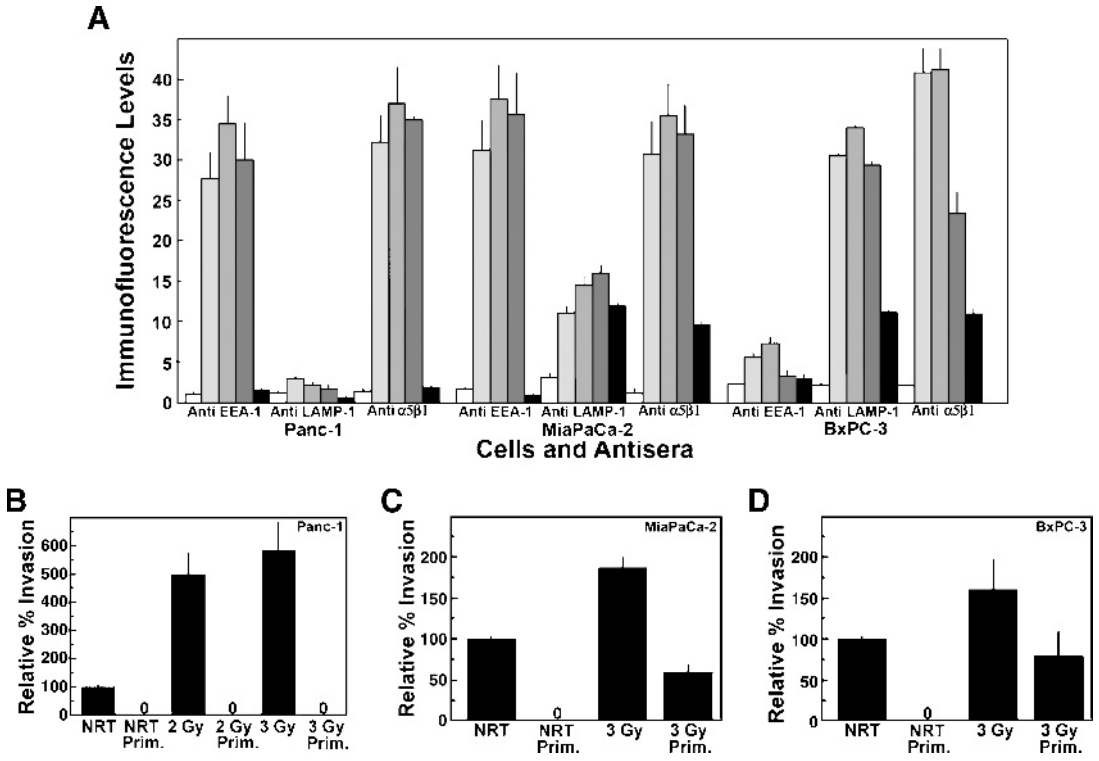

Figure 5. Effects of radiation and primaquine treatment on radiation-induced anti-$\alpha_5\beta_1$, EEA-1, and LAMP-1 immunostaining and on radiation-induced invasion. (A) IF levels of anti–EEA-1, anti–LAMP-1, and anti-$\alpha_5\beta_1$ immunostained cells. *x* axis indicates cells and antisera; *y* axis, mean IF levels (±SEM). Black bars indicate 1 hour after radiation and primaquine treatment; dark gray bars, 4 hours after radiation; light gray bars, 1 hour after radiation; medium gray bars, 2 hours after radiation; white bars, unirradiated cells. Radiation doses: Panc-1, 2 Gy; MiaPaCa-2, 3 Gy; BxPC-3, 3 Gy. Mean IF levels shown (±SEM). All values were obtained from hundreds of cells on four independent plates for each experiment, and each experiment was repeated twice. Significance was set at $P < .05$. (B) Effects of primaquine on radiation-induced Panc-1 invasion *in vitro*. (C) Effects of primaquine in radiation-induced MiaPaCa-2 invasion *in vitro*. (D) Effects of primaquine on radiation-induced BxPC-3 invasion *in vitro*. Panels B, C, and D: *x* axes indicate treatments. NRT indicates no radiation treatment; Prim, primaquine; RT, 1 hour after radiation treatment (Panc-1, 2 Gy; MiaPaCa-2 and BxPC-3, 3 Gy). *y* axes indicate mean percentages of cells invaded (±SD) relative to NRT. Values obtained from quadruplicate plates for each condition, in each of three separate experiments. $P < .05$.

increase on the levels of late endosomes (3.6- to 5.1-fold increase after 1 hour). Consistent with these results, exposure of MiaPaCa-2 cells to primacrine shortly before irradiation reduced neither the levels of radiation-induced late endosomes (3.9-fold increase) nor surface $\alpha_5\beta_1$ (8.1-fold increase), suggesting that late endosomes play a key role in radiation-induced surface $\alpha_5\beta_1$ up-regulation in MiaPaCa-2 cells.

We also determined the effects of primacrine on levels of early and late endosomes, as well as on surface $\alpha_5\beta_1$ in BxPC-3 cells 1, 2, or 4 hours after irradiation. Radiation treatment caused a rapid 15- to 17-fold increase in late endosomes and a 13- to 15-fold up-regulation of surface $\alpha_5\beta_1$ in BxPC-3 (Figure 5*A*) but had a much smaller stimulatory effect on early endosomes (1.5- to 3.4-fold increase).

We next determined the effects of primacrine on radiation-induced invasion. Consistent with its inhibitory effects on early endosomal recycling, primacrine pretreatment completely prevented both background and radiation-induced invasion by Panc-1 cells (Figure 5*B*). In contrast, primacrine pretreatment reduced but did eliminate radiation-induced invasion by MiaPaCa-2 or BxPC-3 cells (Figure 5, *C* and *D*, respectively). In fact, it seemed that, although primacrine was able to prevent invasion by unirradiated MiaPaCa-2 and BxPC-3 cells, it had only a partial effect on the increased invasion observed 1 hour after irradiation. These results are consistent with the significant involvement of late endosomal recycling in radiation-induced $\alpha_5\beta_1$ up-regulation in MiaPaCa-2 and BxPC-3 cells, shown in Figure 5*A*.

Up-regulation of $\alpha_5\beta_1$ and EEA-1 or LAMP-1 IF Staining in Irradiated Panc-1, MiaPaCa-2, and BxPC-3 Tumors

To determine the effects of radiation on $\alpha_5\beta_1$ integrin, as well as on early and late endosome recycling *in vivo*, we analyzed Panc-1–, MiaPaCa-2–, and BxPC-3–derived xenografts for $\alpha_5\beta_1$ integrin, EEA-1, and LAMP-1 immunofluorescence. To equalize any possible effects of the circulation on up-regulation levels, immunofluorescence was quantitated 0 to 75 μm from the edges of the sectioned tumors, as defined by the presence of vasculature and/or visible connective tissue. Effects of radiation on surface $\alpha_5\beta_1$, EEA-1, and LAMP-1 levels and on their colocalization in sectioned Panc-1, MiaPaCa-2, and BxPC-3 tumors are shown in Figure 6. As shown in Figure 6 (*A* and *C*), mean anti-$\alpha_5\beta_1$ immunofluorescence levels were increased significantly, by three- to five-fold ($P < .05$), in irradiated Panc-1, MiaPaCa-2, and BxPC-3 tumors. Mean anti–EEA-1 immunofluorescence levels were also significantly increased in irradiated Panc-1 tumors, relative to unirradiated controls ($P < .05$). A smaller but detectable increase in anti–EEA-1 immunofluorescence was also observed in irradiated MiaPaCa-2 tumors ($P < .05$), but very little increase was observed

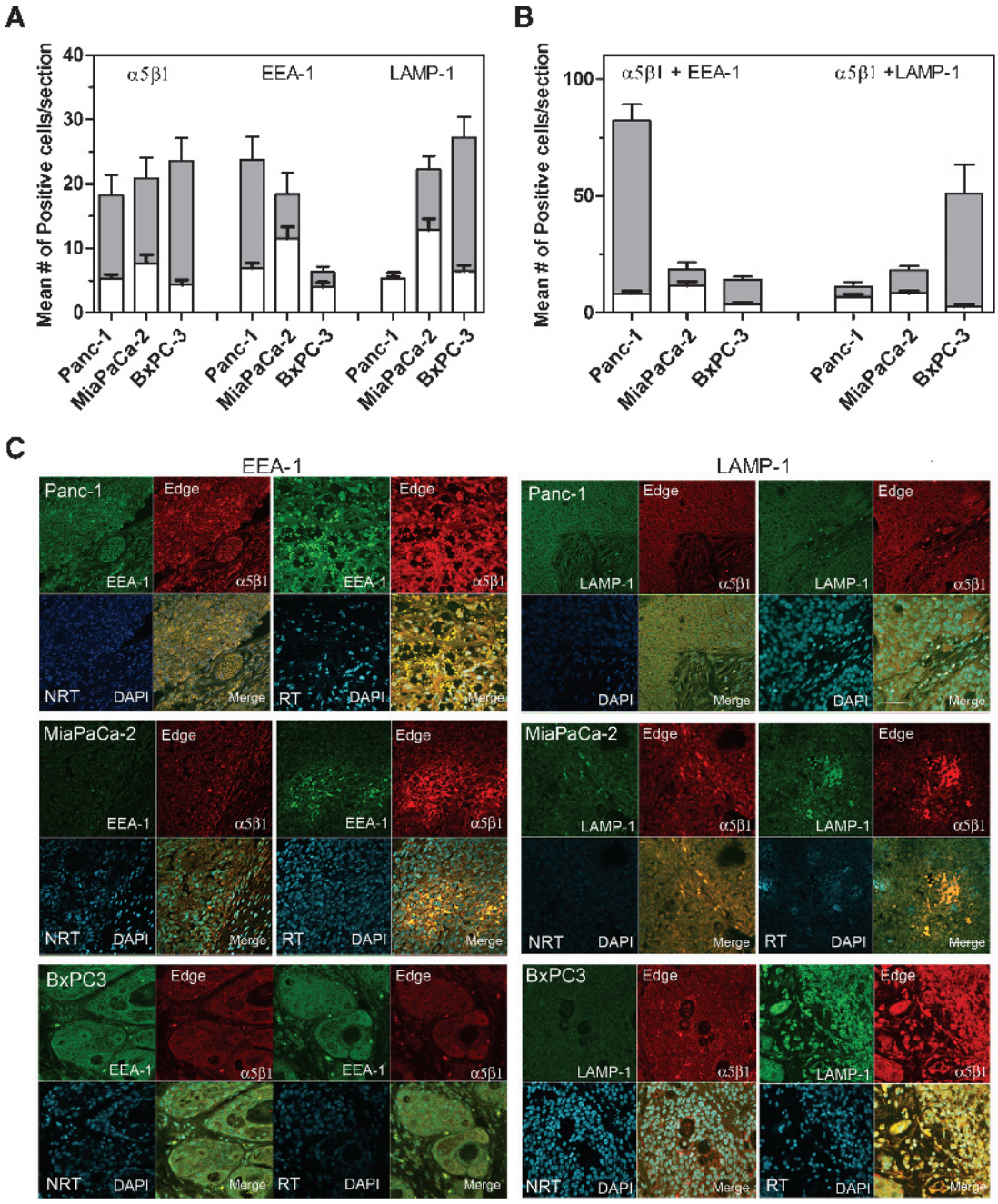

Figure 6. Effects of radiation on $\alpha_5\beta_1$, EEA-1, and LAMP-1 up-regulation and colocalization in Panc-1, MiaPaCa-2, and BxPC-3 tumors in athymic nude mice. (A) Up-regulation of $\alpha_5\beta_1$, EEA-1, or LAMP-1 fluorescent immunostaining in irradiated Panc-1, MiaPaCa-2, and BxPC-3 tumors. *x* axis indicates tumors. Gray bars are sections from irradiated Panc-1, MiaPaCa-2, and BxPC-3 tumors; white bars are sections from unirradiated Panc-1, MiaPaCa-2, and BxPC-3 tumors; white and gray bars are shown as superimposed. *y* axis indicates the mean number of positive cells (±SEM), exhibiting anti-$\alpha_5\beta_1$, anti–EEA-1, or anti–LAMP-1 IF in greater than 70% of the cytoplasmic area for each cell. Each mean value shown was obtained from all cells in 30 sections, each separated by 50 μm, for each of five irradiated and five unirradiated tumors, for a total of 150 sections per tumor. Tumor areas scored were located from 0 to 75 μm from the edges of the tumors, as defined by the presence of microvasculature and/or connective tissue. Significance was set at $P < .05$. (B) Colocalization of upregulated $\alpha_5\beta_1$ and EEA-1 or upregulated $\alpha_5\beta_1$ and LAMP-1 fluorescent immunostaining in irradiated Panc-1, MiaPaCa-2, and BxPC-3 tumors. *x* axis indicates tumors. Bars are shown as superimposed; gray bars are sections from irradiated Panc-1, MiaPaCa-2, or BxPC-3 tumors; white bars are sections from unirradiated Panc-1, MiaPaCa-2, or BxPC-3 tumors. *y* axis indicates mean number of positive cells (±SEM), containing colocalized (yellow), anti-$\alpha_5\beta_1$ and anti–EEA-1, or anti-$\alpha_5\beta_1$ and anti–LAMP-1 immunofluorescence in greater than 70% of the cytoplasmic area for each cell. Each mean value shown was obtained from all cells in 30 sections, each separated by 50 μm, for each of nine irradiated and nine unirradiated tumors, for a total of 150 sections per tumor. Significance was set at $P < .05$. (C) Examples of anti–EEA-1 and anti-$\alpha_5\beta_1$ or anti–LAMP-1 and anti-$\alpha_5\beta_1$ immunostained Panc-1, MiaPaCa-2, or BxPC-3 tumor sections. Sections were photographed at 0 to 75 μm from the edge. $\alpha_5\beta_1$ indicates anti-$\alpha_5\beta_1$ primary MAb; DAPI, nuclear DNA; EEA-1, anti–EEA-1 primary Ab (antiserum); LAMP-1, anti–LAMP-1 primary Ab; NRT, no radiation treatment; RT, radiation treatment (a total of five daily 2-Gy doses).

in irradiated BxPC-3 tumors. In contrast, anti–LAMP-1 immunofluorescence was significantly ($P < .05$) increased in irradiated MiaPaCa-2 and BxPC-3 tumors, but not in Panc-1 tumors, relative to unirradiated controls (Figure 6, *A* and *C*).

We next wished to determine whether $\alpha_5\beta_1$ integrin was colocalized with early endosomes in irradiated tumor xenografts. Hence, we scored tumor cells according to anti–EEA-1 (green) and anti-$\alpha_5\beta_1$ (red) immunofluorescence, as shown by gold fluorescence in greater than 70% of their cytoplasmic volume. We found colocalized $\alpha_5\beta_1$ integrin and EEA-1 to be significantly increased ($P < .05$), by approximately 10-fold, in response to radiation in Panc-1 tumors (Figure 6*B*), consistent with the ability of primacrine to prevent radiation-induced Panc-1 cell invasion (Figure 5). In MiaPaCa-2 tumors, the radiation-induced increase in the mean number of cells with colocalized anti–EEA-1 and anti-$\alpha_5\beta_1$ immunofluorescence was significant ($P < .05$) but smaller than in Panc-1. In irradiated BxPC-3 tumors, the mean number of cells with colocalized anti–EEA-1 and anti-$\alpha_5\beta_1$ immunofluorescence seemed to increase somewhat; however, even after irradiation, the numbers of BxPC-3 tumor cells exhibiting significant anti–EEA-1 immunofluorescence levels were still very low.

The effects of radiation on the levels of colocalized $\alpha_5\beta_1$ integrin and late endosomes were also assessed in the pancreatic tumors. We found that radiation induced an approximately 20-fold increase in BxPC-3 tumors and that this increase was significant ($P < .05$). Furthermore, irradiated MiaPaCa-2 tumors also exhibited a significant increase in colocalized anti-$\alpha_5\beta_1$ and LAMP-1 immunofluorescence ($P < .05$), whereas Panc-1 tumors exhibited no radiation-induced increase in colocalized anti-$\alpha_5\beta_1$ and anti–LAMP-1. These results suggest that late endosomes may play an important role in radiation-induced invasion by MiaPaCa-2 and BxPC-3 tumor cells; but may not be critical to radiation-induced Panc-1 invasion. Radiation-induced $\alpha_5\beta_1$, EEA-1 and LAMP-1 up-regulation in more interior regions (150-300 μm from the vasculature/connective tissue) of irradiated Panc-1, MiaPaCa-2, and BxPC-3 tumors exhibited similar patterns, but the overall levels of up-regulation were not as great (data not shown). These results suggest that, although early endosomes may play a significant role in radiation-induced invasion by Panc-1 tumor cells, late endosomes may be more important in radiation-induced invasion by MiaPaCa-2 and BxPC-3 tumor cells.

Discussion

In this study, we have found that a low dose of ionizing radiation rapidly induces $\alpha_5\beta_1$ integrin–mediated, pFn-dependent invasion by Panc-1, MiaPaCa-2, and BxPC-3 pancreatic cancer cells. Increased invasion was associated with surface $\alpha_5\beta_1$ integrin up-regulation, which occurred by mechanisms including increased α_5 transcription (BxPC-3 and MiaPaCa-2), as well as increased postendocytic recycling of $\alpha_5\beta_1$ from early (Panc-1) or from both early and late endosomes (MiaPaCa-2 and BxPC-3). Our results also indicated that interstitial collagenase MMP-1 is required for radiation-induced invasion by all three pancreatic cancer cell lines, consistent with the key role of MMP-1 in $\alpha_5\beta_1$-mediated invasion by breast and prostate cancer cells, microvascular endothelial cells, fibroblasts, and keratinocytes [7–11]. In support of the requirement for MMP-1 in radiation-induced invasion, we also observed that radiation causes rapid up-regulation of MMP-1 mRNA levels in Panc-1, MiaPaCa-2, and BxPC-3 cells. These findings were further supported by the results of *in vivo* studies indicating that $\alpha_5\beta_1$ is upregulated in response to radiation in Panc-1, MiaPaCa-2, and BxPC-3 xenografts through mechanisms involving early and late endosome recycling of $\alpha_5\beta_1$ integrin.

Because prior studies have demonstrated that $\alpha_5\beta_1$ receptors play key roles in both angiogenic invasion by microvascular endothelial cells and metastatic invasion by breast and prostate cancer cells [7–10], their surface up-regulation in response to radiation could have important consequences in pancreatic cancer, especially concerning the invasive behaviors of surviving cells. This is an important consideration because several studies by us and by others have shown that substantial numbers of Panc-1, MiaPaCa-2, and BxPC-3 cells survive radiation at doses similar to or greater than those used here. For example, 80% of MiaPaCa-2 and 75% of BxPC-3 cells have been shown to survive a 3-Gy dose by clonogenic assay, and a 4-Gy dose has been found to induce apoptosis in only 15% of MiaPaCa-2 and 20% of BxPC-3 cells [26]. Also, a single 7-Gy dose has been shown to reduce Panc-1 clonogenic survival by just 30% [27]. Consistent with these results, a 30-Gy dose induced apoptosis in 7% of Panc-1 cells after 48 hours, as shown by propidium iodide flow cytometry [28]. We have also observed similar clonogenic survival levels in BxPC-3 and MiaPaCa-2 cells, after single doses of 4.0, 5.0, or 6.0 Gy [29,30]. Thus, substantial numbers of Panc-1, MiaPaCa-2, and BxPC-3 cells likely survive and proliferate after receiving the single 2- or 3-Gy dose required for invasion induction.

Consistent with our observations, radiation has been shown to increase surface integrin expression and invasiveness in other types of cancer cells. For example, radiation increased MMP-1 mRNA levels, as well as adhesion, migration, and invasion on type I collagen by human non–small cell lung cancer H1299 cells [31]. Radiation also increased surface levels of $\alpha_5\beta_1$ integrin, and adhesion to fibronectin by COLO-320 human colorectal cancer cells [6]. Radiation, at dosage levels similar to those reported here, has been shown to upregulate both $\alpha_5\beta_1$ integrin and its ligand, fibronectin, specifically in cultured malignant human breast cancer cells. Moreover, a high expression of α_5 integrin gene was found to be significantly associated with a reduced survival in breast cancer patients [32]. A radiation-induced increase in invasion by Panc-1 cells has also been observed [33]. In addition to direct effects on cancer cell invasion, radiation may also stimulate pancreatic cancer cell invasion indirectly, through effects on stromal fibroblasts [34]. It has also been proposed that radiation-induced inflammatory responses might increase invasion of tumor margins by leukocytes; hence, several studies have focused on the effects of radiation on adhesion molecules specifically involved in leukocyte invasion and inflammation [35,36].

The key roles of $\alpha_5\beta_1$ integrin and MMP-1 in invasion and metastasis suggest that an inhibitor specifically targeting the constitutively activated $\alpha_5\beta_1$ integrin receptors of tumor cells and the endothelial cells of their associated vasculature, which mediate MMP-1–dependent angiogenic and metastatic invasion [7–10], might be an efficacious, well-tolerated therapy, which could be used to limit invasion by surviving tumor cells after radiation therapy. We have devised a five-amino-acid peptide that is a potent inhibitor of $\alpha_5\beta_1$ integrin–mediated invasion by metastatic cancer cells. The acetylated, amidated PHSCN peptide, Ac-PHSCN-NH_2 [8], emerged as an invasion inhibitor during structure activity studies of the invasion-inducing PHSRN peptide [11]. The PHSRN sequence of the fibronectin cell binding domain [37,38] is uniquely an $\alpha_5\beta_1$ integrin ligand. In addition to preventing prostate cancer cell invasion and metastasis [8], Ac-PHSCN-NH_2 is also a potent inhibitor of microvascular endothelial cell invasion and angiogenesis [10]. Systemic Ac-PHSCN-NH_2 prevented disease progression

for prolonged periods in several preclinical models [8,39–41]. As ATN-161, systemic Ac-PHSCN-NH_2 was also a well-tolerated efficacious monotherapy in a phase 1 clinical trial, where 0.5- to 5.0-mg/kg dosage levels prevented disease progression for 4 to 14 months in more than 30% of patients receiving it [42]. Recently, a highly potent derivative of the PHSCN peptide, formed by attaching eight PHSCN moieties to a polylysine dendrimer multiantigenic protein, or MAP, to make Ac-PHSCNGGK-MAP, was found to be 1000- to 1900-fold more efficacious than Ac-PHSCN-NH_2 at blocking basement membrane invasion by DU 145 and PC-3 human prostate cancer cells or by SUM149PT and MDA-MB-231 human breast cancer cells *in vitro*, as well as extravasation and lung colony formation *in vivo* [43,44]. Thus, $\alpha_5\beta_1$ integrin may be a fruitful target for the prevention of metastatic as well as radiation-induced invasion. These results suggest that, in addition to preventing disease progression, inhibition of $\alpha_5\beta_1$ integrin–mediated invasion by systemic Ac-PHSCN-NH_2 or Ac-PHSCNGGK-MAP therapy might also reduce local invasion during radiotherapy for pancreatic cancer patients.

Acknowledgments

The authors thank Mary Davis for assistance with this article.

References

[1] Iacobuzio-Donahue CA, Fu B, Yachida S, Luo M, Abe H, Henderson CM, Vilardell F, Wang Z, Keller JW, Banerjee P, et al. (2009). DPC4 gene status of the primary carcinoma correlates with patterns of failure in patients with pancreatic cancer. *J Clin Oncol* **27**, 1806–1813.

[2] Cardenes HR, Chiorean EG, Dewitt J, Schmidt M, and Loehrer P (2006). Locally advanced pancreatic cancer: current therapeutic approach. *Oncologist* **11**, 612–623.

[3] Chang BW, Siccion E, and Saif MW (2010). Updates in locally advanced pancreatic cancer. Highlights from the "2010 ASCO Annual Meeting". Chicago, IL, USA. June 4-8, 2010. *JOP* **11**, 313–316.

[4] Baluna RG, Eng TY, and Thomas CR (2006). Adhesion molecules in radiotherapy. *Radiat Res* **166**, 819–831.

[5] Wild-Bode C, Weller M, Rimner A, Dichgans J, and Wick W (2001). Sublethal irradiation promotes migration and invasiveness of glioma cells: implications for radiotherapy of human glioblastoma. *Cancer Res* **61**, 2744–2750.

[6] Meineke V, Gilbertz KP, Schilperoort K, Cordes N, Sendler A, Moede T, and van Beuningen D (2002). Ionizing radiation modulates cell surface integrin expression and adhesion of COLO-320 cells to collagen and fibronectin *in vitro*. *Strahlenther Onkol* **178**, 709–714.

[7] Jia Y, Zeng ZZ, Markwart SM, Rockwood KF, Ignatoski KM, Ethier SP, and Livant DL (2004). Integrin fibronectin receptors in matrix metalloproteinase-1–dependent invasion by breast cancer and mammary epithelial cells. *Cancer Res* **64**, 8674–8681.

[8] Livant DL, Brabec RK, Pienta KJ, Allen DL, Kurachi K, Markwart S, and Upadhyaya A (2000). Anti-invasive, antitumorigenic, and antimetastatic activities of the PHSCN sequence in prostate carcinoma. *Cancer Res* **60**, 309–320.

[9] Zeng Z-Z, Jia YF, Hahn NJ, Markwart SM, Rockwood KF, and Livant DL (2006). Role of focal adhesion kinase and phosphatidylinositol 3′-kinase in integrin fibronectin receptor–mediated, matrix metalloproteinase-1 dependent invasion by metastatic prostate cancer cells. *Cancer Res* **66**, 8091–8099.

[10] Zeng ZZ, Yao H, Staszewski ED, Rockwood KF, Markwart SM, Fay KS, Spalding AC, and Livant DL (2009). $\alpha_5\beta_1$ integrin ligand PHSRN induces invasion and α_5 mRNA in endothelial cells to stimulate angiogenesis. *Transl Oncol* **2**, 8–20.

[11] Livant DL, Brabec RK, Kurachi K, Allen DL, Wu Y, Haaseth R, Andrews P, Ethier SP, and Markwart S (2000). The PHSRN sequence induces extracellular matrix invasion and accelerates wound healing in obese diabetic mice. *J Clin Invest* **105**, 1537–1545.

[12] Roberts MS, Woods AJ, Dale TC, Van Der Sluijs P, and Norman JC (2004). Protein kinase B/Akt acts via glycogen synthase kinase 3 to regulate recycling of $\alpha_v\beta_3$ and $\alpha_5\beta_1$ integrins. *Mol Cell Biol* **24**, 1505–1515.

[13] Murk JL, Stoorvogel W, Kleijmeer MJ, and Geuze HJ (2002). The plasticity of multivesicular bodies and the regulation of antigen presentation. *Semin Cell Dev Biol* **13**, 303–311.

[14] Tan MH, Nowak NJ, Loor R, Ochi H, Sandberg AA, Lopez C, Pickren JW, Berjian R, Douglass HO Jr, and Chu TM (1986). Characterization of a new primary human pancreatic tumor line. *Cancer Invest* **4**, 15–23.

[15] Lieber M, Mazzetta J, Nelson-Rees W, Kaplan M, and Todaro G (1975). Establishment of a continuous tumor-cell line (panc-1) from a human carcinoma of the exocrine pancreas. *Int J Cancer* **15**, 741–747.

[16] Wu M, Arimura GK, and Yunis AA (1977). Purification and characterization of a plasminogen activator secreted by cultured human pancreatic carcinoma cells. *Biochemistry* **16**, 1908–1913.

[17] Cheng S, Tada M, Hida Y, Asano T, Kuramae T, Takemoto N, Hamada J, Miyamoto M, Hirano S, Kondo S, et al. (2008). High MMP-1 mRNA expression is a risk factor for disease-free and overall survivals in patients with invasive breast carcinoma. *J Surg Res* **146**, 104–109.

[18] Albertin G, Ruggero M, Guidolin D, and Nussdorfer GG (2006). Gene silencing of human RAMP2 mediated by short-interfering RNA. *Int J Mol Med* **18**, 531–535.

[19] Zhou S-Y, Lu Y-X, Yao H, and Owyang C (2008). Spatial organization of neurons in the dorsal motor nucleus of the vagus synapsing with intragastric cholinergic and nitric oxide/VIP neurons in the rat. *Am J Physiol Gastrointest Liver Physiol* **294**, G1201–G1209.

[20] Li Y, Wu X, Yao H, and Owyang C (2005). Secretin activates vagal primary afferent neurons in the rat: evidence from electrophysiological and immunohistochemical studies. *Am J Physiol Gastrointest Liver Physiol* **289**, G745–G752.

[21] Chakraborty TR, Ng L, and Gore AC (2003). Age-related changes in estrogen receptor β in rat hypothalamus: a quantitative analysis. *Endocrinology* **144**, 4164–4171.

[22] Oo TF, Henchcliffe C, James D, and Burke RE (1999). Expression of c-*fos*, c-*jun*, and c-*jun* N-terminal kinase (JNK) in a developmental model of induced apoptotic death in neurons of the substantia nigra. *J Neurochem* **72**, 557–564.

[23] Ng T, Shima D, Squire A, Bastiaens PI, Gschmeissner S, Humphries MJ, and Parker PJ (1999). PKCα regulates β_1 integrin–dependent cell motility through association and control of integrin traffic. *EMBO J* **18**, 3909–3923.

[24] Spang A (2009). On the fate of early endosomes. *Biol Chem* **390**, 753–759.

[25] van Weert AW, Geuze HJ, Groothuis B, and Stoorvogel W (2000). Primaquine interferes with membrane recycling from endosomes to the plasma membrane through a direct interaction with endosomes which does not involve neutralisation of endosomal pH nor osmotic swelling of endosomes. *Eur J Cell Biol* **79**, 394–399.

[26] Chung HW, Wen J, Lim JB, Bang S, Park SW, and Song SY (2009). Radiosensitization effect of STI-571 on pancreatic cancer cells *in vitro*. *Int J Radiat Oncol Biol Phys* **75**, 862–869.

[27] Konduri S, Colon J, Baker CH, Safe S, Abbruzzese JL, Abudayyeh A, Basha MR, and Abdelrahim M (2009). Tolfenamic acid enhances pancreatic cancer cell and tumor response to radiation therapy by inhibiting survivin protein expression. *Mol Cancer Ther* **8**, 533–542.

[28] Song X, Wang H, Logsdon CD, Rashid A, Fleming JB, Abbruzzese JL, Gomez HF, and Evans DB (2011). Overexpression of receptor tyrosine kinase Axl promotes tumor cell invasion and survival in pancreatic ductal adenocarcinoma. *Cancer* **117**, 734–743.

[29] Morgan MA, Parsels LA, Kollar LE, Normolle DP, Maybaum J, and Lawrence TS (2008). The combination of epidermal growth factor receptor inhibitors with gemcitabine and radiation in pancreatic cancer. *Clin Cancer Res* **14**, 5142–5149.

[30] Morgan MA, Parsels LA, Zhao L, Parsels JD, Davis MA, Hassan MC, Arumugarajah S, Hylander-Gans L, Morosini D, Simeone DM, et al. (2010). Mechanism of radiosensitization by the Chk1/2 inhibitor AZD7762 involves abrogation of the G_2 checkpoint and inhibition of homologous recombinational DNA repair. *Cancer Res* **70**, 4972–4981.

[31] Tsutsumi K, Tsuda M, Yazawa N, Nakamura H, Ishihara S, Haga H, Yasuda M, Yamazaki R, Shirato H, Kawaguchi H, et al. (2009). Increased motility and invasiveness in tumor cells that survive 10 Gy irradiation. *Cell Struct Funct* **34**, 89–96.

[32] Nam JM, Onodera Y, Bissell MJ, and Park CC (2010). Breast cancer cells in three-dimensional culture display an enhanced radioresponse after coordinate targeting of integrin $\alpha_5\beta_1$ and fibronectin. *Cancer Res* **70**, 5238–5248.

[33] Qian LW, Mizumoto K, Urashima T, Nagai E, Maehara N, Sato N, Nakajima M, and Tanaka M (2002). Radiation-induced increase in invasive potential of

human pancreatic cancer cells and its blockade by a matrix metalloproteinase inhibitor, CGS27023. *Clin Cancer Res* **8**, 1223–1227.

[34] Hwang RF, Moore T, Arumugam T, Ramachandran V, Amos KD, Rivera A, Ji B, Evans DB, and Logsdon CD (2008). Cancer-associated stromal fibroblasts promote pancreatic tumor progression. *Cancer Res* **68**, 918–926.

[35] Hallahan DE, Staba-Hogan MJ, Virudachalam S, and Kolchinsky A (1998). X-ray–induced P-selectin localization to the lumen of tumor blood vessels. *Cancer Res* **58**, 5216–5220.

[36] Kawana A, Shioya S, Katoh H, Tsuji C, Tsuda M, and Ohta Y (1997). Expression of intercellular adhesion molecule-1 and lymphocyte function–associated antigen-1 on alveolar macrophages in the acute stage of radiation-induced lung injury in rats. *Radiat Res* **147**, 431–436.

[37] Aota S, Nagai T, and Yamada KM (1991). Characterization of regions of fibronectin besides the arginine-glycine-aspartic acid sequence required for adhesive function of the cell-binding domain using site-directed mutagenesis. *J Biol Chem* **266**, 15938–15943.

[38] Mould AP, Askari JA, Aota SI, Yamada KM, Irie A, Takada Y, Mardon HJ, and Humphries MJ (1997). Defining the topology of integrin $\alpha_5\beta_1$-fibronectin interactions using inhibitory anti-α_5 and anti-β_1 monoclonal antibodies. Evidence that the synergy sequence of fibronectin is recognized by the amino-terminal repeats of the α_5 subunit. *J Biol Chem* **272**, 17283–17292.

[39] Khalili P, Arakelian A, Chen G, Plunkett ML, Beck I, Parry GC, Donate F, Shaw DE, Mazar AP, and Rabbani SA (2006). A non–RGD-based integrin binding peptide (ATN-161) blocks breast cancer growth and metastasis *in vivo*. *Mol Can Ther* **5**, 2271–2280.

[40] Stoeltzing O, Liu W, Reinmuth N, Fan F, Parry GC, Parikh AA, McCarty MF, Bucana CD, Mazar AP, and Ellis LM (2003). Inhibition of integrin $\alpha_5\beta_1$ function with a small peptide (ATN-161) plus continuous 5-FU infusion reduces colorectal liver metastases and improves survival in mice. *Int J Cancer* **104**, 496–503.

[41] van Golen KL, Bao L, Brewer GJ, Pienta KJ, Kamradt JM, Livant DL, and Merajver SD (2002). Suppression of tumor recurrence and metastasis by a combination of the PHSCN sequence and the antiangiogenic compound tetrathiomolybdate in prostate carcinoma. *Neoplasia* **4**, 373–379.

[42] Cianfrocca ME, Kimmel KA, Gallo J, Cardoso T, Brown MM, Hudes G, Lewis N, Weiner L, Lam GN, Brown SC, et al. (2006). Phase 1 trial of the antiangiogenic peptide ATN-161 (Ac-PHSCN-NH_2), a β integrin antagonist, in patients with solid tumours. *Br J Cancer* **94**, 1621–1626.

[43] Yao H, Veine D, Fay K, Staszewski E, Zeng Z-Z, and Livant D (2011). The PHSCN dendrimer as a more potent inhibitor of human breast cancer cell invasion, extravasation, and lung colony formation. *Breast Cancer Res Treat* **125**, 363–375.

[44] Yao H, Veine DM, Zeng ZZ, Fay KS, Staszewski ED, and Livant DL (2010). Increased potency of the PHSCN dendrimer as an inhibitor of human prostate cancer cell invasion, extravasation, and lung colony formation. *Clin Exp Metastasis* **27**, 173–184.